Type 2 Innate Lymphoid Cells Protect against Colorectal Cancer Progression and Predict Improved Patient Survival

Qiutong Huang, Nicolas Jacquelot, Adele Preaudet, Soroor Hediyeh-zadeh, Fernando Souza-Fonseca-Guimaraes, Andrew N.J. McKenzie, Philip M. Hansbro, Melissa J. Davis, Lisa A. Mielke, Tracy L. Putoczki and Gabrielle T. Belz
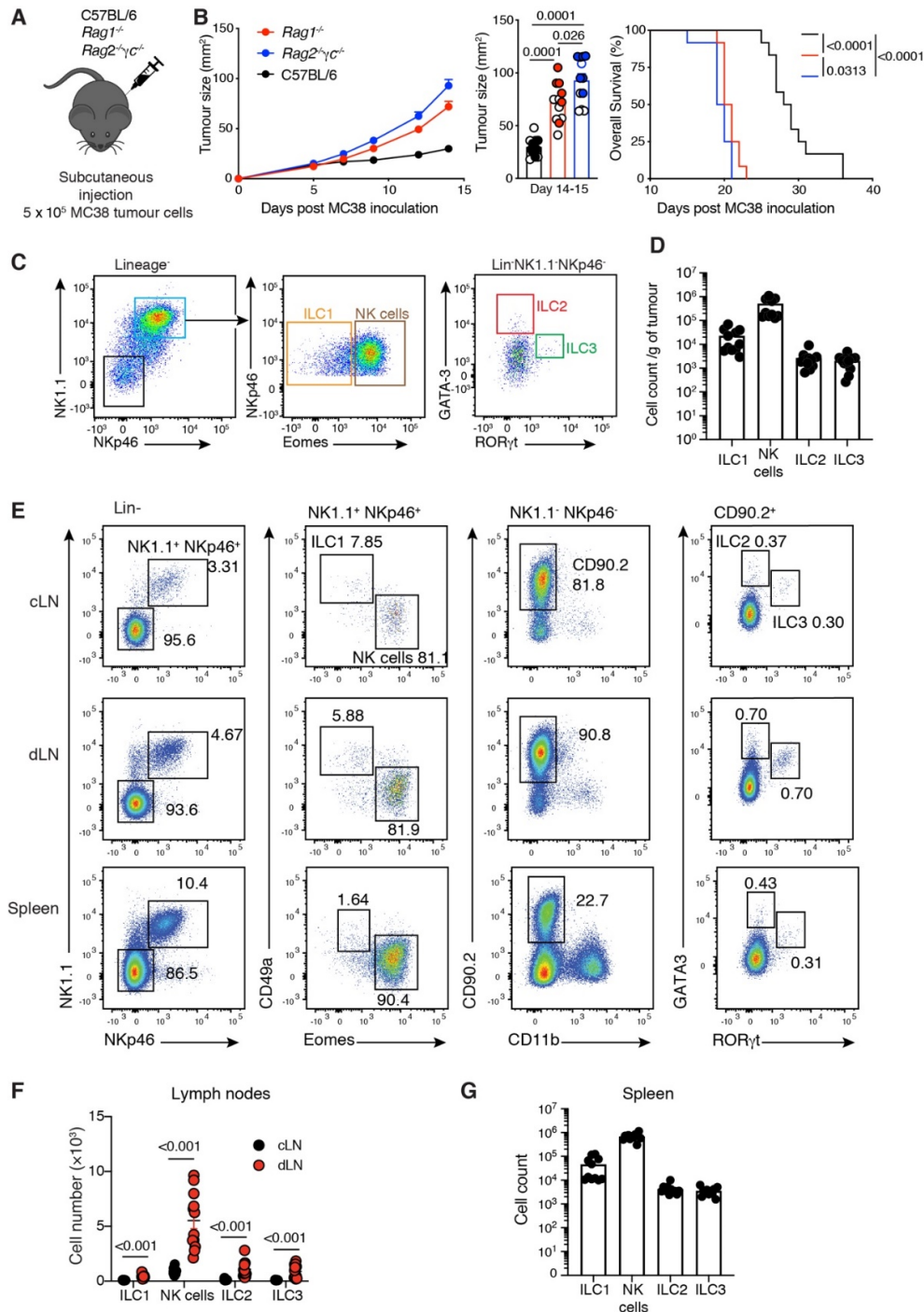
Figure S1. Enumeration of ILC subsets in MC38 tumour-bearing mice. A. Experimental approach to induction of tumours in immunocompetent C57BL/6, *Rag1*^{-/-} (deficient in adaptive immune cells) and *Rag2*^{-/-}*γc*^{-/-} (deficient in both innate and adaptive immune cells). **B**. C57BL/6, *Rag1*^{-/-} and *Rag2*^{-/-}*γc*^{-/-} mice were inoculated subcutaneously with MC38 tumour cells. Tumour growth curves over time (left panel), tumour size at day 14-15 post tumour cell inoculation (middle panel) and survival (right panel) are shown. Each dot represents one mouse, closed circle for females, open circles for males. Data show mean ± s.e.m and are pooled from 2 independent experiments with 6 mice/group/experiment (C57BL/6, *n*=12 mice; *Rag1*^{-/-}, *n*=12 mice; *Rag2*^{-/-}*γc*^{-/-}, *n*=12 mice). Analyses were performed using the TumGrowth software. **C-G**. Flow cytometric analyses of tumour-infiltrating ILCs. **C**. Representative gating strategies are shown for identification of NK cells, ILC1, ILC2 and ILC3. **D**. Enumeration of tumour-infiltrating ILC isolated at day 16 post MC38 cell inoculation of tumour-bearing C57BL/6 mice. Each dot represents one mouse, closed circle for females. Data show mean ± s.e.m and are pooled from 2 independent experiments with 6 mice/group/experiment. Live NK cells were identified as follow: CD45^{+}CD3^{-}TCRβ^{-}CD19^{-}NK1.1^{+}NKp46^{+}Eomes^{+}; ILC1 as NK1.1^{+}NKp46^{+}Eomes^{-}; ILC2 as NK1.1^{-}NKp46^{-}CD90.2^{+}CD49a^{-}CD11b^{-}GATA3^{+}; and ILC3 as NK1.1^{-}NKp46^{-}CD90.2^{+}CD49a^{-}CD11b^{-}RORγt^{+}. **E**. Representative gating strategy to identify ILCs in contralateral lymph nodes (cLN), tumour-draining lymph nodes (dLN), and spleen. Live NK cells were identified as follow: CD45^{+}CD3^{-}TCRβ^{-}CD19^{-} NK1.1^{+}NKp46^{+}Eomes^{+}; ILC1 as NK1.1^{+}NKp46^{+}Eomes^{-}; ILC2 as NK1.1^{-}NKp46^{-}CD90.2^{+}CD49a^{-}CD11b^{-}GATA3^{+}; and ILC3 as NK1.1^{-}NKp46^{-}CD90.2^{+}CD49a^{-}CD11b^{-}RORγt^{+}. **F-G**. Enumeration of ILC1, NK cells, ILC2 and ILC3 isolated from (cLN), (dLN) (**F**) and spleen (**G**) of tumour-bearing C57BL/6 mice at day 16 post MC38 cell inoculation. ILCs were identified as in **E**. Each dot represents one mouse, closed circle for females. Data show mean ± s.e.m and are pooled from 2 independent experiments with 6 mice/group/experiment. Statistical analyses were performed using unpaired Student's *t* tests and *p* values are indicated.
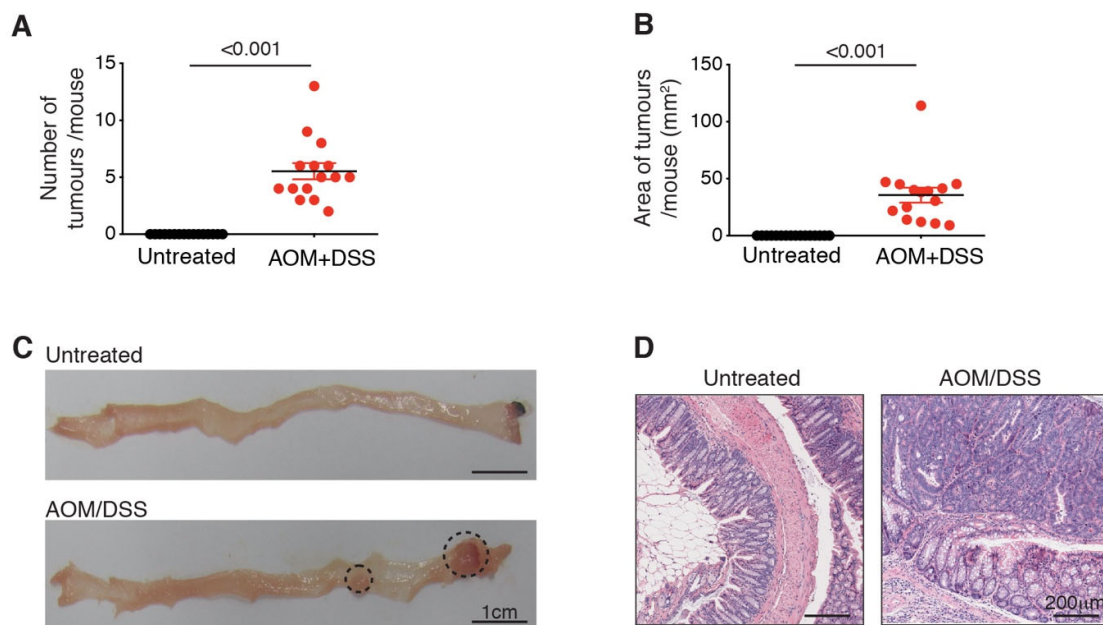

Figure S2. Incidence of CRC tumours in AOM DSS-treated mice. A-B. Number (**A**) and area of tumours (mm[2], **B**) per mouse in C57BL/6 mice treated or not with AOM+DSS. Each dot represents one mouse, closed circle for females. Data show the mean ± s.e.m (*n*=2-3 mice/experiment) pooled from four independent experiments. Statistical differences were analysed using the Mann-Whitney nonparametric test. *p* values are indicated. **C**. Representative whole mount images of colons from C57BL/6 mice treated, or untreated, with AOM+DSS. Images are representative of 15-16 mice/genotype analysed in four separate experiments. Dotted lines indicate tumour size and location. Scale bar, 1 cm. **D**. Representative images of colon sections stained with Hematoxylin & Eosin which were collected from naïve and AOM+DSS treated C57BL/6 mice. Images are representative of >10 mice/genotype. Scale bar, 200 μm.
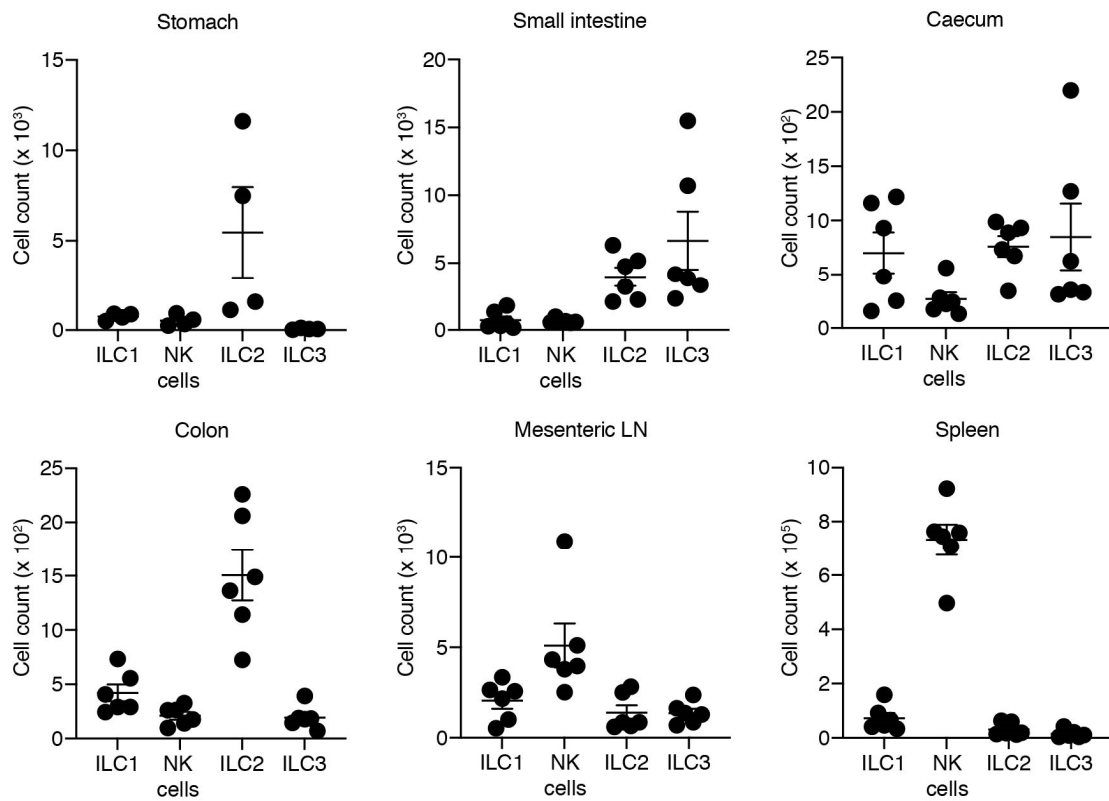
Figure S3. ILC composition within the intestinal tract, mesenteric lymph nodes and spleen of untreated C57BL/6 mice. Enumeration of the ILC subsets in the lamina propria of the stomach, small intestine, caecum and colon as well as in the mesenteric lymph nodes (LN) and spleen of naive C57BL/6 mice. ILC1 were identified as follow: $CD45^+CD3^-NK1.1^+NKp46^+Eomes^-$; NK cells as $NK1.1^+NKp46^+Eomes^+$; ILC2 as $CD127^+GATA3^+$; and ILC3 as $CD127^+ROR\gamma t^+$. Data show the mean $\pm$ s.e.m. Data are pooled from three independent experiments (*n*=2 mice/experiment) except for stomach (one experiment in which each data point represents the average of three stomachs pooled together). Statistical differences are reported in Table S2.
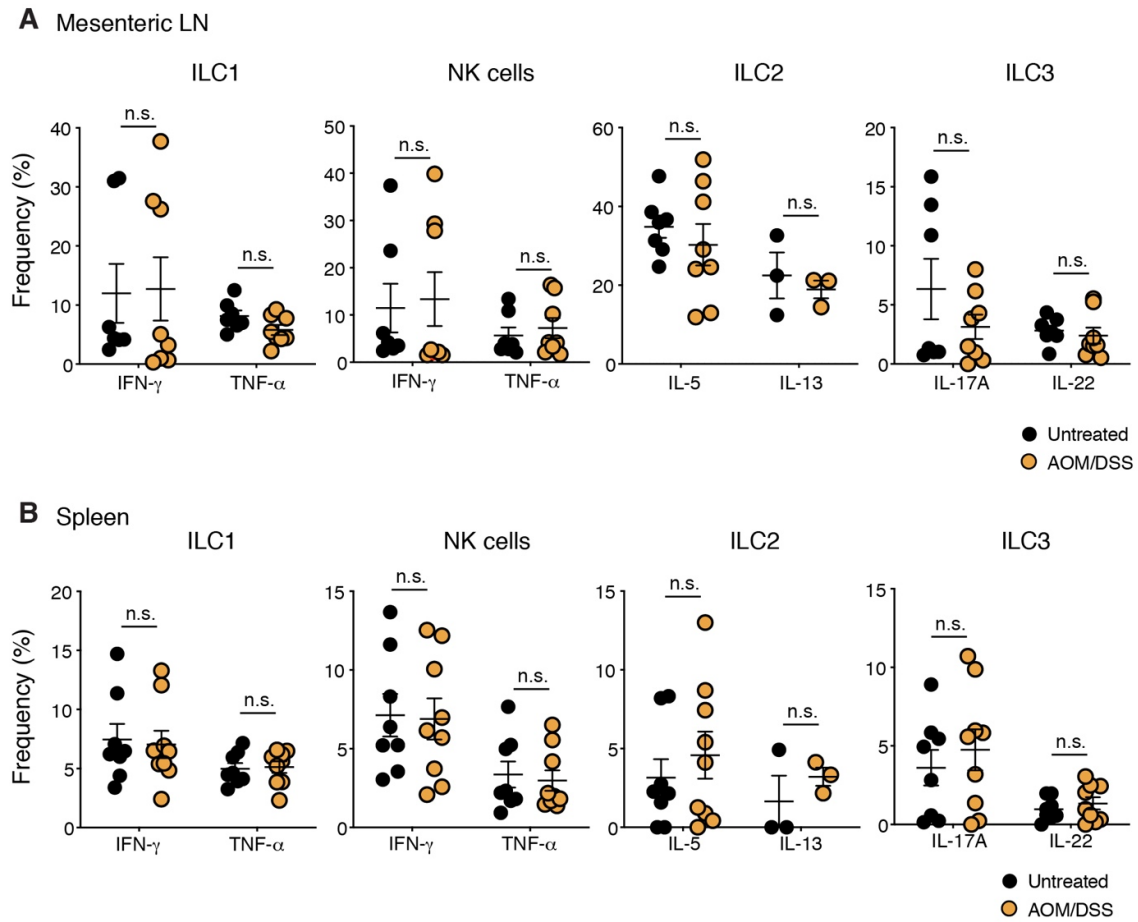
Figure S4. The ILC cytokine production in spleen and mesenteric lymph nodes is not influenced during CAC progression. A-**B**. Intracellular staining flow-cytometric analyses of TNF-α, IFN-γ, IL-5, IL-13, IL-17A and IL-22 cytokine production by ILC1, NK cells, ILC2 and ILC3 isolated from the mesenteric lymph nodes (**A**) and spleens (**B**) after short-term restimulation with PMA, ionomycin in the presence of Golgi Stop and Golgi Plug. Cells were stimulated for 4 hours before staining. Frequency of cytokine-producing ILC isolated from the mesenteric lymph nodes (**A**) and spleen (**B**) of untreated and AOM DSS-treated mice. Each dot represents one mouse. Data show the mean ± s.e.m. IL-13 data is from one experiment, all other data is pooled from four independent experiments (*n*=2-3 mice/genotype/experiment). Statistical differences were analysed using the Mann-Whitney nonparametric test. n.s., not significant.
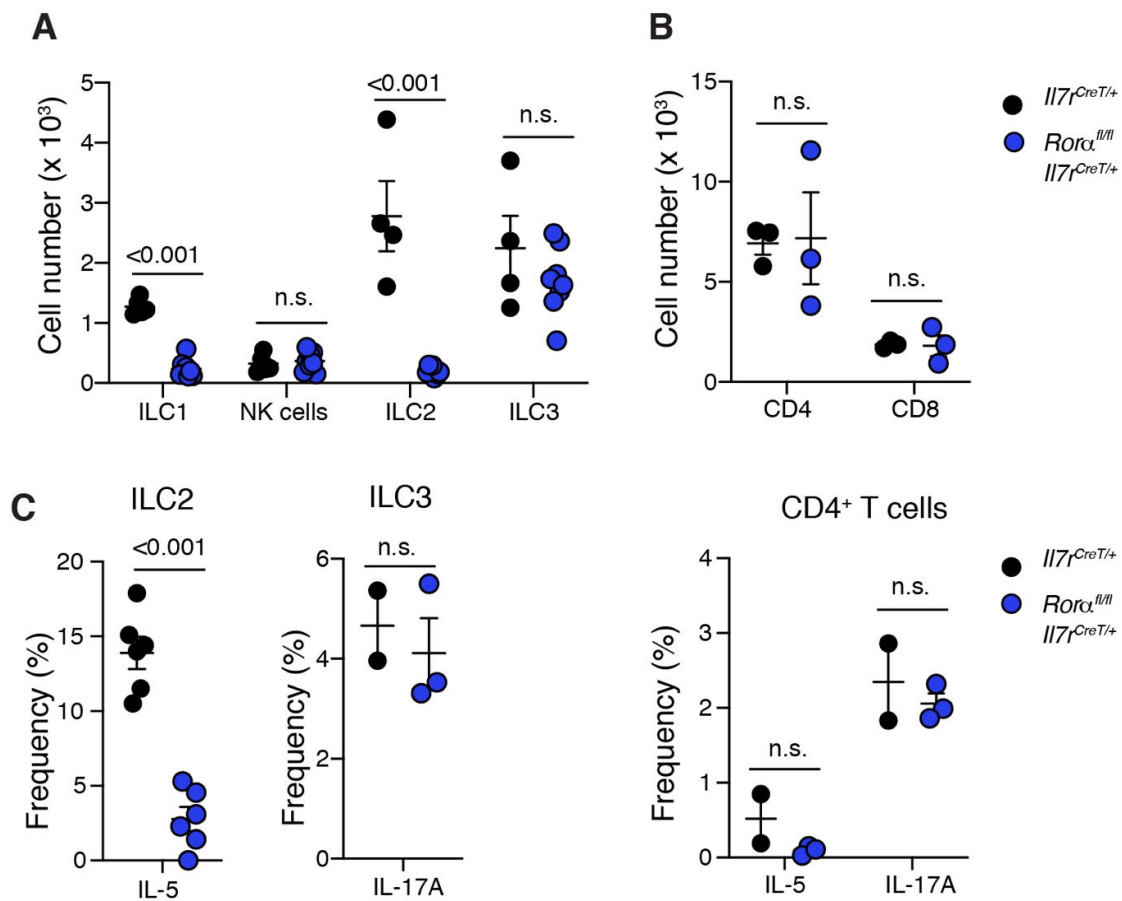
Figure S5. Deletion of RORα results in loss of ILC1 and ILC2 but not T cells or other ILC subsets at steady-state. A-B. Enumeration of ILC (**A**) and CD4+ and CD8+ T cell (**B**) subsets isolated from the colon of naïve 8 weeks old *Il7r$^{Cre\ T/+}$* and *Rorα$^{fl/fl}$Il7r$^{Cre\ T/+}$* mice. Data show the mean ± s.e.m. ILC2 data is pooled from two independent experiments, ILC3 and T cell data are from one experiment (*n*=2-4 mice/genotype/experiment). **C**. Frequency of IL-5 and IL-17A cytokine producing ILC2, ILC3 and CD4+ T cells. Data show the mean ± s.e.m. ILC2 data is pooled from two independent experiments, ILC3 and CD4+ T cell data are from one experiment (*n*=2-4 mice/genotype/experiment). **A-C**. Each dot represents one mouse. Statistical significance was determined using an unpaired Student's *t* test *p* values are indicated. n.s., not significant.

Figure S6. Deletion of RORα results in loss of ILC1 but not cytokine production or other lymphoid subsets during CAC. A. Enumeration of non-ILC2 ILC subsets isolated from the colon of AOM+DSS treated *Il7r^{Cre T/+}* and *Rorα^{fl/fl}Il7r^{Cre T/+}* mice. Data show the mean ± s.e.m. ILC3 data is pooled from two independent experiments, ILC1 and NK cell data are from one experiment (*n*=3 mice/genotype/experiment). **B**. Number of colonic CD4+ and CD8+ T cells of AOM+DSS treated *Il7r^{Cre T/+}* and *Rorα^{fl/fl}Il7r^{Cre T/+}* mice. Data show the mean ± s.e.m and are pooled from two independent experiments (*n*=3 mice/genotype/experiment). **C**. Frequency of IFN-γ cytokine producing ILC1 and NK cells and IL-17A/IL22 producing ILC3. Data show the mean ± s.e.m. ILC3 data is pooled from two independent experiments, ILC1 and NK cell data is from one experiment (*n*=2-4 mice/genotype/experiment) **A**-**C**. Each dot represents one mouse. Statistical significance was determined using an unpaired Student's *t* test *p* values are indicated. n.s., not significant.
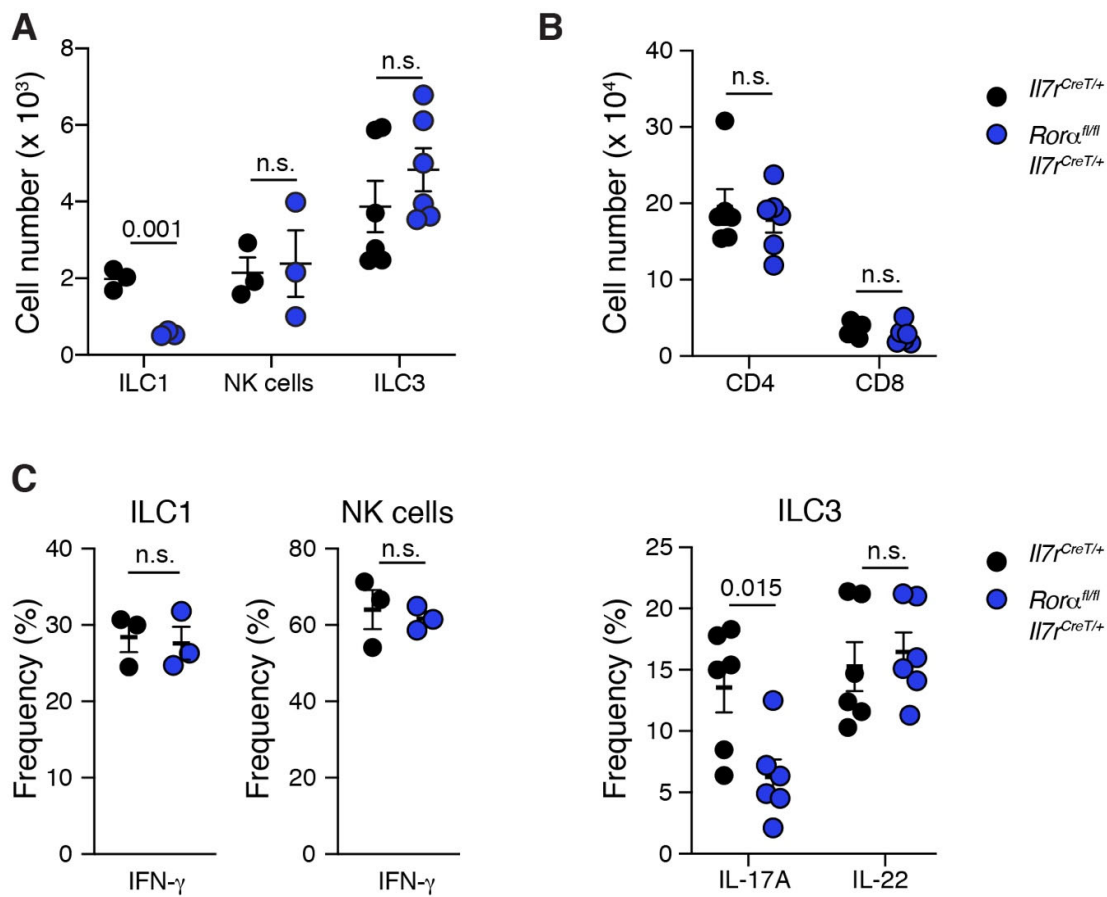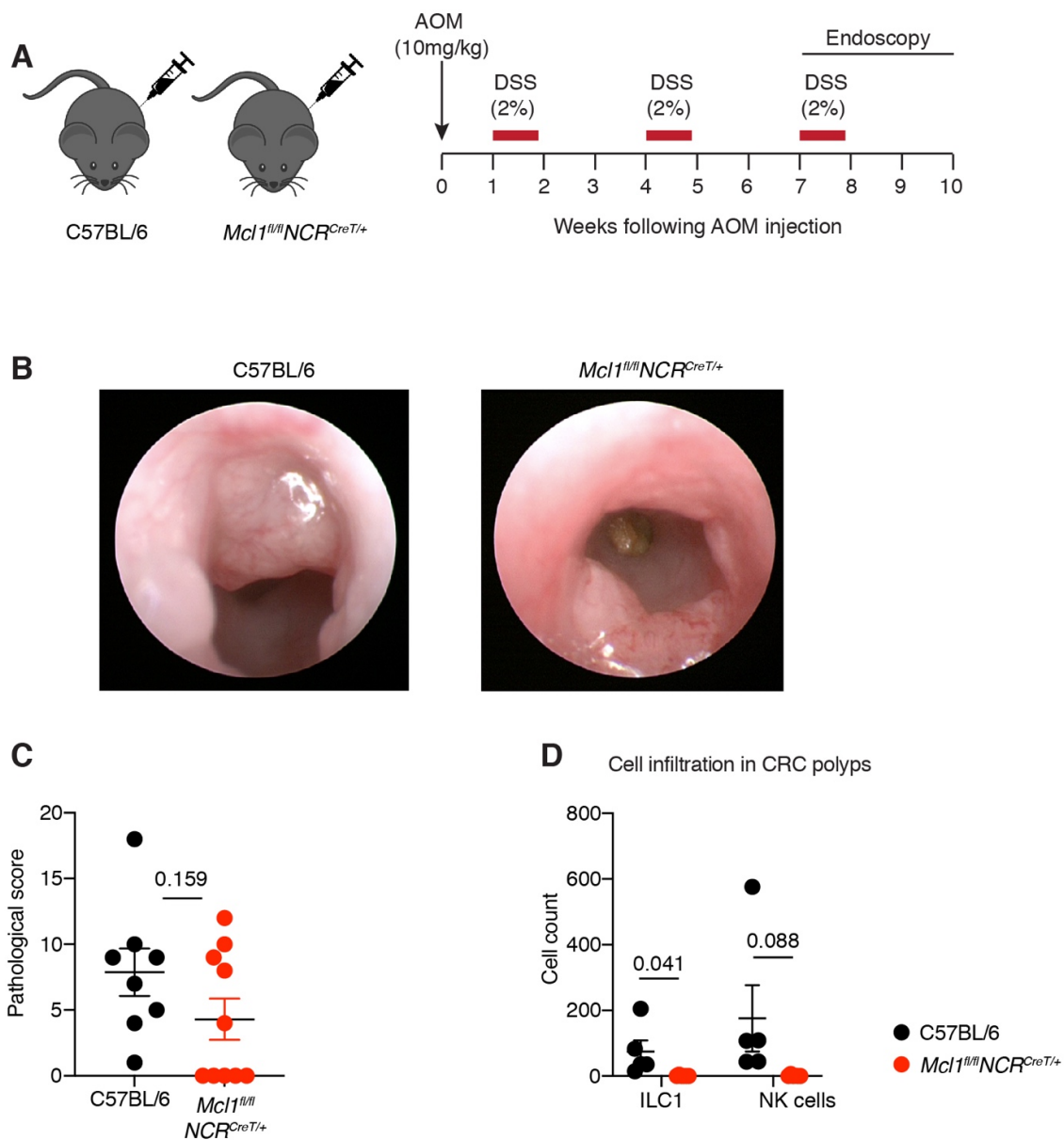
Figure S7. Loss of ILC1 and NK cells does not impact CAC development. A. Schematic illustration of the AOM/DSS treatment protocol. C57BL6 and *Mcl1^fl/fl^NCR^CreT/+^* mice injected with AOM (10mg/kg, i.p) followed by three 5-day cycles of 2% (w/v) DSS *ad libitum* in their drinking water separated by two weeks of normal water between each cycle. Colonic tumours developed between 7-10 weeks after the initial commencement of treatment. **B**. Endoscopic images of AOM/DSS-treated C57BL6 and *Mcl1^fl/fl^NCR^CreT/+^* mice. Images are representative of 8 to 10 mice/genotype. **C**. Pathological score of colons from C57BL6 or *Mcl1^fl/fl^NCR^CreT/+^* mice treated with AOM+DSS. **D**. FACS enumeration of group 1 innate lymphoid cell (ILC1 – Eomes^-^CD49a^+^; NK cells – Eomes^+^CD49a^-^) infiltration in colons of C57BL/6 and *Mcl1^fl/fl^NCR^CreT/+^* mice treated with AOM+DSS. Each dot represents one mouse. Data show the mean $\pm$ s.e.m (*n*=5-10 mice/genotype). Statistical differences were analysed using unpaired Student's *t* test. *p*-values are indicated.

Table S1. Longitudinal, cross-sectional and survival analyses from MC38 tumour-bearing C67BL/6, *Rag1*^{-/-} and *Rag2*^{-/-}*γc*^{-/-} for TumGrowth analysis.

Longitudinal analysis

Type II ANOVA

	F test (KR)	F test (S)	LR test	Wald test
Time x Treat	88.64 (d.f.=2/63.7), *p*<<0.0001	88.76 (d.f.=2/74.6), *p*<<0.0001	75.49 (d.f.=2), *p*<<0.0001	177.52 (d.f.=2), *p*<<0.0001
Time	527.42 (d.f.=1/39.7), *p*<<0.0001	527.64 (d.f.=1/36.7), *p*<<0.0001	101.58 (d.f.=1), *p*<<0.0001	527.64 (d.f.=1), *p*<<0.0001
Treat	9.17 (d.f.=2/34.1), *p*<0.0007	9.24 (d.f.=2/401.0), *p*<0.0001	15.82 (d.f.=2), *p*<0.0004	18.48 (d.f.=2), *p*<<0.0001

Selected pairwise comparisons

p-value adjustment: Holm

Largest	Smallest	Contrast	Df	*p*-value	*p*-value adjusted
Rag1^{-/-}	**C57BL/6**	0.089 [0.072;0.106]	55.18	<0.0001	<0.0001
Rag2^{-/-}*γc*^{-/-}	**C57BL/6**	0.099 [0.082;0.117]	63.02	<0.0001	<0.0001
Rag2^{-/-}*γc*^{-/-}	**Rag1**^{-/-}	0.010 [-0.008;0.029]	81.48	0.2661	0.2661

Cross-sectional analysis

ANOVA

	Likelihood ratio test	F test	Kruskall-Wallis
Treat	48.12 (d.f.=2), *p*<<0.0001	61.16 (d.f.=2), *p*<<0.0001	25.40 (d.f.=2), *p*<<0.0001

Selected pairwise comparisons

p-value adjustment: Holm

Group 1	Group 2	Difference	*p*-value	*p*-value adjusted	Wilcox *p*-value	Wilcox *p*-value adjusted
Rag1^{-/-}	**C57BL/6**	41.917 [28.333;55.500]	<0.0001	<0.0001	<0.0001	0.0001
Rag2^{-/-}*γc*^{-/-}	**C57BL/6**	62.958 [47.417;78.500]	<0.0001	<0.0001	<0.0001	0.0001
Rag2^{-/-}*γc*^{-/-}	**Rag1**^{-/-}	21.042 [2.089;39.995]	0.0097	0.0097	0.0260	0.0260

Survival analysis (*Rag1*^{-/-} as a reference)

ANOVA

	Likelihood ratio test	Wald test	Log-Rank test
Treat	46.29 (d.f.=2), *p*<<0.0001	4.38 (d.f.=2), *p*<0.1120	36.97 (d.f.=2), *p*<<0.0001

Hazard ratios

p-value adjustment: Holm

Covariate	Hazard ratio	*p*-value	*p*-value adjusted	Log-Rank *p*-value	Log-Rank *p*-value adjusted
C57BL/6	-Inf [-Inf;Inf]	0.8440	0.8440	<0.0001	<0.0001
Rag2^{-/-}*γc*^{-/-}	2.556 [1.057;6.183]	0.0373	0.0745	0.0313	0.0313

Table S2. ANOVA analysis of ILC subsets in gastrointestinal organs at steady-state.

Comparison	Stomach	Small intestine	Caecum	Colon	Mesenteric LN	Spleen
ILC1 *vs.* NK	>0.9999	<u>0.0173</u>	0.3003	0.5646	0.2650	0.4347
ILC1 *vs.* ILC2	0.7133	<u>0.0042</u>	>0.9999	0.5181	>0.9999	>0.9999
ILC1 *vs.* ILC3	0.2697	0.0766	>0.9999	0.3968	>0.9999	0.1649
NK *vs.* ILC2	0.2697	>0.9999	0.0539	<u>0.0042</u>	<u>0.0105</u>	<u>0.0151</u>
NK *vs.* ILC3	0.7133	<u>0.0225</u>	0.1335	>0.9999	<u>0.0219</u>	<u>0.0004</u>
ILC2 *vs.* ILC3	<u>0.0022</u>	>0.9999	>0.9999	<u>0.0023</u>	>0.9999	>0.9999

Underlined numbers represent *p*-values of comparisons with statistically significant difference.

Table S3. ILC2 gene signature.

Feature	Weight	Feature	Weight	Feature	Weight
IL2	0.206869	FLT3LG	0.00111423	IFI16	0
CCR4	0.0863433	RUNX3	0.00089958	EWSR1	0
ECSIT	0.0735243	SMAD3	0.00074262	ITK	0
IL10RA	0.055715	CD53	0.00071255	TNFSF10	0
LRRN3	0.0531323	CD44	0.00071142	CYFIP2	0
IL17RB	0.0462906	JAK2	0.00065083	ILF3	0
ITGAE	0.0461633	CCR1	0.00061332	CYLD	0
IL1RL1	0.0404291	STAT1	0.00060124	MAP3K7	0
KLRG1	0.0362019	CD81	0.00059675	IFITM2	0
CSF2	0.0236164	IRF4	0.00056124	PIK3CD	0
CD74	0.0232307	TNFSF14	0.00055953	NUP107	0
GATA3	0.0224158	IL7R	0.0005343	ITGAL	0
TNFRSF4	0.0218217	HAVCR2	0.00052931	TFRC	0
CD27	0.0206863	EGR1	0.00050366	TRAF6	0
PRKCE	0.0206544	LYN	0.00046362	IRF7	0
OSM	0.0199132	IRAK1	0.00046162	CD63	0
PDCD1	0.0154011	MAPK1	0.00034388	IFI35	0
FOS	0.00974204	LY9	0.00033311	CLU	0
POU2F2	0.00847504	BCL2L1	0.00029227	CD28	0
CASP1	0.00750729	RELA	0.00026883	FAS	0
IL15RA	0.00635427	CDKN1A	0.00022799	ATG5	0
JAK3	0.00620136	ABCB1	0.00019413	CD37	0
CD3EAP	0.00594586	ATF2	0.00017671	TYK2	0
NFKBIA	0.00586913	REPS1	0.00016272	RIPK2	0
ISG15	0.00576078	IL2RA	0.000162	LAMP2	0
TRAF3	0.00471944	CD96	0.00012582	ST6GAL1	0
ADA	0.00421412	YTHDF2	0.00012306	IRF1	0
NCF4	0.0038821	ATG16L1	0.00012085	DDX58	0
IL2RG	0.00353999	ANP32B	0.00010744	ENTPD1	0
LIF	0.00337071	TBK1	0.00010289	STAT4	0
CASP8	0.00319852	STAT3	8.36E-05	GTF3C1	0
IFNAR1	0.0030248	ENG	7.33E-05	SMAD2	0
GPI	0.00229326	PSEN2	3.87E-05	MAF	0
C1QBP	0.00215396	ANXA1	2.94E-05	CASP3	0
CHUK	0.00170722	PTPRC	6.07E-06	INPP5D	0
CXCR6	0.00146083	TXNIP	0	MAPK3	0
IL2RB	0.00144123	CD2	0	PTGS2	0

Feature	Weight	Feature	Weight	Feature	Weight
TNFRSF18	0.00133321	*KIT*	0	*IL21R*	0
PLAUR	0.00113747	*CD84*	0	*NT5E*	0
Feature	**Weight**	**Feature**	**Weight**	**Feature**	**Weight**
NFATC1	0	*TOLLIP*	0	*IL18RAP*	-0.00238245
IRF2	0	*BCL10*	0	*CD164*	-0.00244962
NOTCH1	0	*IL17RA*	0	*BST2*	-0.0029268
MAP4K2	0	*IFNAR2*	0	*STAT6*	-0.00312513
MAP2K4	0	*IL12RB1*	-3.20E-06	*MAPK14*	-0.00335746
BATF	0	*ZAP70*	-3.02E-05	*TNFSF4*	-0.00347132
NFATC3	0	*IFNGR1*	-4.11E-05	*TCF7*	-0.00397718
ATG10	0	*BAX*	-4.31E-05	*CD3G*	-0.0062911
MAP3K5	0	*HLA-DQA1*	-4.75E-05	*NRP1*	-0.00657612
PSEN1	0	*TNFRSF9*	-4.95E-05	*IL18R1*	-0.00660455
ICAM1	0	*TRAF2*	-6.00E-05	*ITGA5*	-0.0070242
STAT5B	0	*ATG7*	-7.26E-05	*TXK*	-0.00755759
STAT2	0	*ICOS*	-8.01E-05	*IRAK2*	-0.00774614
MAPK8	0	*CSF1*	-8.99E-05	*NFATC2*	-0.00803036
TNFRSF11A	0	*CCR2*	-0.00010368	*TNFAIP3*	-0.00854714
MAVS	0	*TFE3*	-0.00011479	*TIGIT*	-0.0087403
CREB1	0	*IL16*	-0.00013147	*TICAM1*	-0.00895162
IRF3	0	*PECAM1*	-0.00013353	*IRF8*	-0.0100038
IKBKE	0	*BCL2*	-0.00013441	*ISG20*	-0.010305
PRKCD	0	*CD48*	-0.00017676	*TNFRSF1A*	-0.0115377
THBS1	0	*TANK*	-0.00020269	*MEF2C*	-0.0119517
TNFRSF1B	0	*LRP1*	-0.00021933	*IRF5*	-0.0119688
EP300	0	*APP*	-0.00024874	*SLAMF1*	-0.0121617
SIGIRR	0	*CCL5*	-0.00027321	*RORC*	-0.0132505
IL11RA	0	*CCND3*	-0.00029067	*LGALS3*	-0.0139224
FADD	0	*ITGB2*	-0.00033562	*MYD88*	-0.0146959
IGF2R	0	*SELPLG*	-0.00044161	*CTSH*	-0.0150875
PSMD7	0	*CTSS*	-0.0004603	*SPN*	-0.0154769
IKBKB	0	*ATF1*	-0.00049572	*LCK*	-0.0157092
CEBPB	0	*MAP3K1*	-0.00050973	*JAK1*	-0.0157398
CD47	0	*UBC*	-0.00084905	*CXCR4*	-0.0213308
ABL1	0	*DUSP4*	-0.00110906	*IGF1R*	-0.0239232
REL	0	*CD247*	-0.00113715	*DUSP6*	-0.0245169
NLRC5	0	*NLRP3*	-0.00119608	*DOCK9*	-0.0253211
MAP2K1	0	*LCP1*	-0.00134211	*IL1R1*	-0.027627
PIK3CG	0	*ITGA6*	-0.00148169	*CTSW*	-0.0294796
HLA-DMA	0	*CD3D*	-0.00154358	*CCR7*	-0.0352911
MAP2K2	0	*TNFSF11*	-0.00176661	*FCER1G*	-0.0356495
TP53	0	*CD83*	-0.00186132	*TNFSF8*	-0.107785
ATM	0	*IL6R*	-0.00216832	*CCR6*	-0.156758
CARD11	0	*IRAK4*	-0.00236336	*KLRB1*	-0.17907
				KLRC1	-0.208495